The natural axis of transmitter receptor distribution in the human cerebral cortex

Alexandros Goulas[a,1], Jean-Pierre Changeux[b,c,1], Konrad Wagstyl[d,e,f], Katrin Amunts[g,h], Nicola Palomero-Gallagher[g,h,i,j], and Claus C. Hilgetag[a,k]

[a]Institute of Computational Neuroscience, University Medical Center Hamburg-Eppendorf, 20246 Hamburg, Germany; [b]Communications Cellulaires, Collège de France, 75005 Paris, France; [c]CNRS UMR 3571, Institut Pasteur, 75724 Paris, France; [d]McGill Centre for Integrative Neuroscience, Montréal Neurological Institute, Montréal, Canada QC H3A 2B4; [e]Department of Psychiatry, University of Cambridge, Cambridge CB2 0SZ, United Kingdom; [f]Wellcome Trust Centre for Neuroimaging, University College London, London WC1N 3AR, United Kingdom; [g]Institute of Neuroscience and Medicine (INM-1), Research Centre Jülich, 52425 Jülich, Germany; [h]C. and O. Vogt Institute for Brain Research, University Hospital Düsseldorf, Heinrich Heine University Düsseldorf, 40225 Düsseldorf, Germany; [i]Department of Psychiatry, Psychotherapy, and Psychosomatics, Medical Faculty, Rheinisch-Westfälische Technische Hochschule (RWTH) Aachen, 52074 Aachen, Germany; [j]Jülich Aachen Research Alliance (JARA)-Translational Brain Medicine, Aachen, Germany; and [k]Department of Health Sciences, Boston University, Boston, MA 02215

Contributed by Jean-Pierre Changeux, December 9, 2020 (sent for review October 1, 2020; reviewed by Javier DeFelipe, Moritz Helmstaedter, and Basilis (Vasileios) Zikopoulos)

Transmitter receptors constitute a key component of the molecular machinery for intercellular communication in the brain. Recent efforts have mapped the density of diverse transmitter receptors across the human cerebral cortex with an unprecedented level of detail. Here, we distill these observations into key organizational principles. We demonstrate that receptor densities form a natural axis in the human cerebral cortex, reflecting decreases in differentiation at the level of laminar organization and a sensory-to-association axis at the functional level. Along this natural axis, key organizational principles are discerned: progressive molecular diversity (increase of the diversity of receptor density); excitation/inhibition (increase of the ratio of excitatory-to-inhibitory receptor density); and mirrored, orderly changes of the density of ionotropic and metabotropic receptors. The uncovered natural axis formed by the distribution of receptors aligns with the axis that is formed by other dimensions of cortical organization, such as the myelo- and cytoarchitectonic levels. Therefore, the uncovered natural axis constitutes a unifying organizational feature linking multiple dimensions of the cerebral cortex, thus bringing order to the heterogeneity of cortical organization.

cortical organization | unifying principles | molecular diversity

Transmitter receptors are essential for cellular communication, since they are the molecular elements responsible for the responsiveness of cells to distinct types of neurotransmitters. Such a key role has naturally attracted concerted efforts that aim to map and elucidate the role of receptors in a plethora of neurobiological phenomena, ranging from cellular to cognitive processes, with important ramifications for understanding pathologies involving disturbances at the receptor level and drug design (1–7). Positron emission tomography of the human brain can offer a coarse mapping of the distribution of certain receptors, useful for modeling receptor dynamics in the human brain (8) and understanding the pathogenesis of brain disorders at the molecular level (9). While densities for some receptors can be measured in humans with positron emission tomography, for instance, for serotonin (10), there are no suitable positron-emission tomography tracers that can map a plethora of key receptors in living humans in a safe way (e.g., for NMDA). Furthermore, the number of different receptor types that can be examined in a single individual is very small. In vitro quantitative receptor autoradiography of receptor densities has been used for a broad range of key transmitter receptors and offers spatial resolution suitable for uncovering details pertaining to the laminar architecture of the cerebral cortex (7, 11, 12). Moreover, receptor autoradiography reflects quantitative, neurobiologically interpretable measurements. Recent efforts have mapped the distribution of a broad range of transmitter receptors in multiple cortical areas across different laminar compartments (6, 7, 13). These advancements also pose the challenge of compressing these raw observations into a parsimonious set of comprehensible, key organizational principles.

Building on recent endeavors (7), here, we distill key organizational principles of the transmitter receptor distribution of the human cerebral cortex. We highlight an axis of maximum variance of the receptor distribution across the cortex. This natural axis ranges from sensory to association areas of the cerebral cortex. The arrangement of areas along this axis also entails three organizational principles. First, progressive molecular diversity is observed, that is, an increase of the diversity of receptor densities when proceeding from one end of the axis (sensory areas) to the other end of the axis (association areas). Second, progressive excitation/inhibition ratio, that is, the increase of the ratio of excitatory-to-inhibitory receptor density, is also observed along the same direction along the natural axis. Third, progressive, mirrored changes of the density of ionotropic and metabotropic receptors are observed; that is, the density of metabotropic receptors increases when proceeding from sensory

Significance

Communication between cells in the brain relies on different types of transmitter receptors. Can we uncover organizational principles that harness the diversity of such signatures across the brain? We focus on the human cerebral cortex and demonstrate that the distribution of receptors forms a natural axis that stretches from association to sensory areas. Moreover, traversing this axis entails changes in the diversity, excitability, and mirrored density that reflect a basic division in receptor types, that is, ionotropic and metabotropic receptors. The unraveled principles offer explanatory depth for diverse phenomena and entail concrete, testable predictions.

Author contributions: A.G. designed research; A.G., J.-P.C., K.W., K.A., N.P.-G., and C.C.H. performed research; N.P.-G. contributed new reagents/analytic tools; A.G. analyzed data; A.G. wrote the paper; J.-P.C. contributed to the conception of the core theme of the study; and J.-P.C., K.W., K.A., N.P.-G., and C.C.H. provided detailed feedback and suggestions on the draft version of the paper.

Reviewers: J.D., Instituto Cajal (CSIC) and Universidad Politécnica de Madrid; M.H., Max Planck Institute for Brain Research; and B.Z., Boston University School of Medicine, Program in Neuroscience, Boston University.

The authors declare no competing interest.

[1]To whom correspondence may be addressed. Email: a.goulas@uke.de or changeux@noos.fr.

This article contains supporting information online at https://www.pnas.org/lookup/suppl/doi:10.1073/pnas.2020574118/-/DCSupplemental.

Published January 15, 2021.

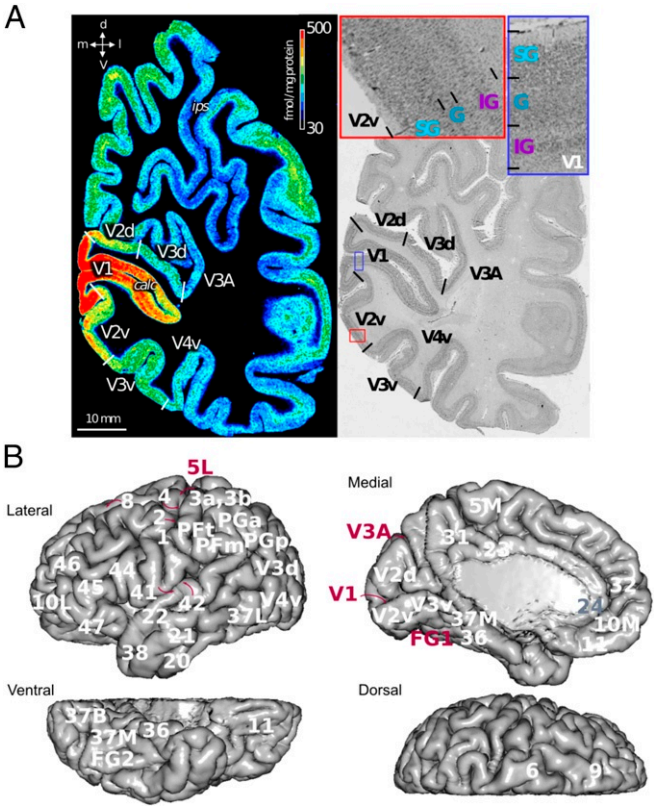

Fig. 1. In vitro receptor autoradiography for estimation of transmitter receptor densities. (*A*) Example of coronal sections through a human brain hemisphere, revealing the density of muscarinic M2 receptors (*Left*) and the distribution of cell bodies (*Right*) for multiple visual areas. Adapted from ref. 7, which is licensed under CC BY 4.0. (*B*) Summary of cortical areas for which laminar transmitter receptor measurements were carried out in ref. 7. G, granular; IG, infragranular; SG, supragranular.

to association areas, while the density of ionotropic receptors is mirrored, thus decreasing along this direction. The aforementioned principles manifest in a laminar-wise fashion, showcasing the importance of uncovering organizational principles at a fine spatial resolution. Moreover, the uncovered receptor-based natural axis aligns with the spatially ordered changes of the cerebral cortex at other levels of architecture, such as the myelo- and cytoarchitectonic levels, in agreement with classic and more recent studies. Our results generate concrete testable predictions that are pertinent to cognitive, computational, and comparative neuroscience.

Results

We analyzed the previously collected data of transmitter receptor densities across a wide range of areas of the human cerebral cortex (7). Density for multiple excitatory, inhibitory, ionotropic, and metabotropic receptors has been measured: glutamate (AMPA, NMDA, kainate), GABA ($GABA_A$, $GABA_A$/BZ, $GABA_B$), acetylcholine (muscarinic M1, M2, M3, nicotinic a_4b_2), noradrenaline (a_1, a_2), serotonin (5-HT_{1A}, 5-HT_2), and dopamine (D_1). Data were acquired in a laminar-wise fashion summarized in densities for granular, infragranular, and supragranular layers. For the receptor autoradiographical incubation protocols used and overall densitometric analytical procedure, see ref. 7. An exemplary section is shown in Fig. 1*A*.

Uncovering the Natural Axis of Transmitter Receptor Density. As a first step, we assembled the receptor density profile of each cortical area, that is, the density measured in each area for each of the aforementioned receptors in granular (G), infragranular (IG), and supragranular (SG) layers. Note that due to the agranular character (lack of the granular layer) of area 24, the only area with this feature in the set of the 44 cortical areas analyzed in ref. 7 (Fig. 1*B*), this area was not included in the analysis, to have a consistent profile with IG, G, and SG measurements for all areas. Inclusion of area 24 and analysis based only on measurements on IG and SG layers led to qualitatively similar results. We aimed at uncovering the trajectory across which most variance of receptor density manifests. To this end, we applied principal component analysis (PCA) to the receptor density profile of all cortical areas. The arrangement of cortical areas across PC1 unveiled a sensory-to-association axis (PC1, accounting for 28% of the variance) and PC2 was driven by the "outlier" character of areas 6 and 4, separating them from the rest of cortical areas (PC2, accounting for 22% of the variance) (Fig. 2). Note that here the terms "association" and "sensory" are not used to denote strict categories for grouping cortical areas. Instead, the terms are used to denote the broad character of areas that span the two extreme ends of the natural axis. In other words, the current results underline the natural axis as a continuum (or gradient) of receptor density variations and not as a discrete set of categories. The biplot simultaneously depicts the observations, that is, cortical areas (denoted with circles tagged with the names of each area), and the features, that is, laminar-wise receptor densities (arrows tagged with the names of each receptor and corresponding laminar compartment), in the PCA space (Fig. 2). Therefore, the biplot allows deciphering what receptor density measurements drive the segregation of cortical areas across the PCA space. Here, we focus on PC1, which explains the largest amount of variance and is, thus, referred to as the primary natural axis of receptor distribution. We use the term "natural axis" to denote the arrangement of cortical areas based on their intrinsic, neurobiological properties, here, the laminar distribution and density of transmitter receptors. Thus, this axis of organization is "natural," in the sense that it does not rely on or require an imposed stereotaxic space and the related terminology, e.g., dorsal–ventral, anteroposterior, etc.

Certain insights into the receptor signatures that segregate cortical areas along the primary natural axis can be discerned in the biplot (Fig. 2). First, receptor density of the IG layers is more prominent in segregating association areas from sensory areas along the natural axis (note the concentration of loadings related to IG measurements with magenta color in the left part of the biplot). Second, the biplot reveals a striking segregation along the natural axis with respect to the glutamate receptors AMPA and NMDA. NMDA is prominent on the sensory-related end of the natural axis, while AMPA is prominent in the association-related end. Third, the biplot reveals the distinctive receptor signatures of sensory areas, that is, the prominent role of the $GABA_A$, a_2, m_2, and D1 receptors in visual sensory areas, segregating them from association areas (Fig. 2). Note that a figure with scores and coefficients plotted separately is provided in *SI Appendix*, Fig. S1.

We subsequently aimed at distilling organizational principles that are not readily discernable from the biplot. Specifically, we estimated the diversity of receptor density of each cortical area as the Shannon entropy of the receptor profile of each area. Entropy was calculated as H = −sum(N*log(N))/log(M), where N is the normalized receptor profile of the area with each entry denoting each normalized receptor density value, with normalized values expressed as the ratio of each receptor density to the maximum receptor density value observed for this receptor across all areas, and M denoting the total number of features of the profile, that is, 45 (densities for 15 receptors for G, IG, and SG layers), and log is the natural logarithm (hence, entropy was normalized to the [0 1] interval).

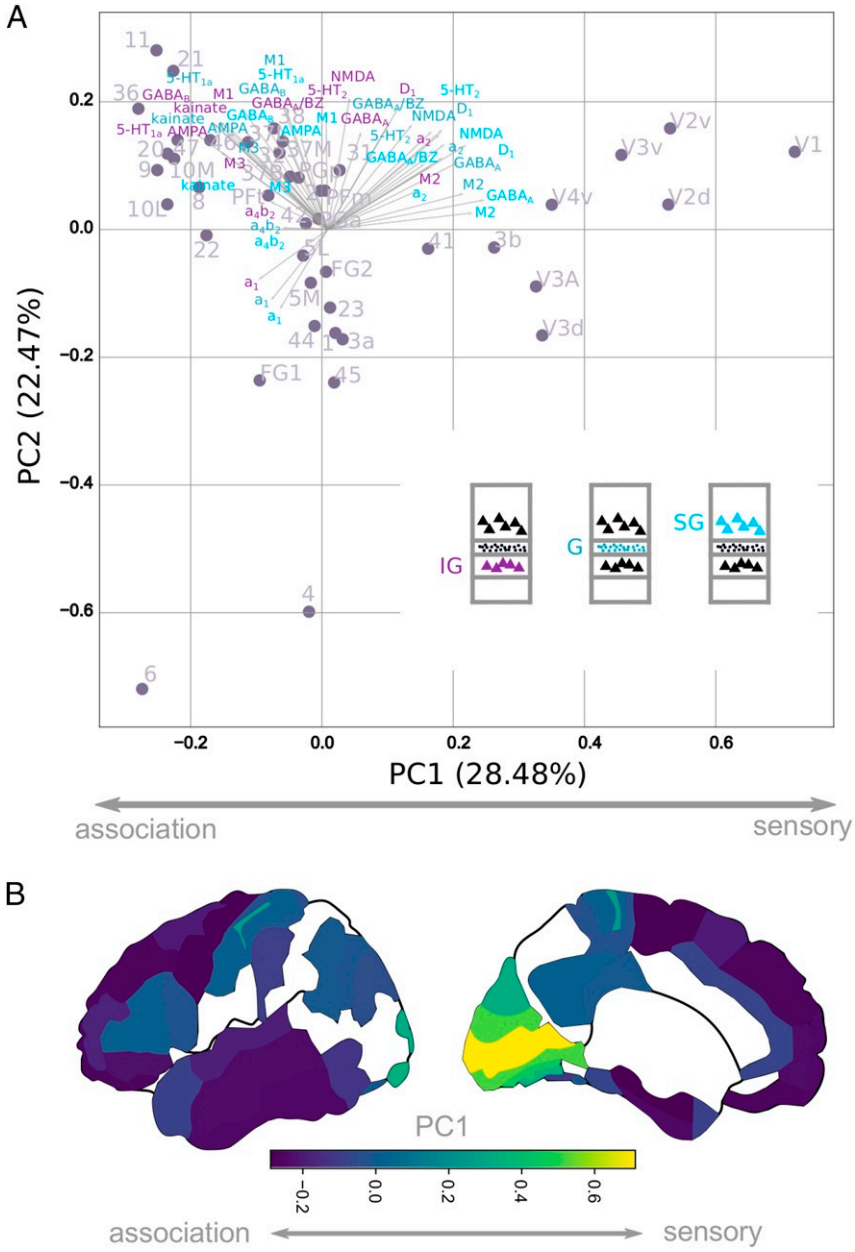

Fig. 2. The natural axis of transmitter receptor density distribution. (*A*) PC1 reveals the distribution of the areas along an axis explaining most of the receptor density variance across cortical areas. The axis stretches from sensory to association areas. We refer to this axis (PC1) as the primary natural axis of transmitter receptor density distribution. Note that here, the terms "association" and "sensory" denote the broad character of areas that span the two extreme ends of the natural axis and that these terms can harbor further subcategories. In this context, association refers to nonsensory areas. Our results emphasize the ordering of cortical areas along the natural axis and, thus, the used binary categories serve only as approximate indicators of the character of cortical areas at the opposite ends of the natural axis. Note that different receptor densities across different laminar compartments, depicted as the PCA coefficients, have a more prominent role in the arrangement of different area constellations along the natural axis. For instance, receptor density of the IG layers is more prominent in association areas and NMDA in the primary areas, while AMPA is prominent in association areas. Finally, a distinctive profile for primary areas is highlighted, that is, prominence of density of the $GABA_A$, a_2, M2, and D1 receptors. (*B*) The natural axis rendered in a surface map of the human cortex. Colors correspond to the PC1 values. Note the association to sensory arrangement of areas along the natural axis.

We also estimated the excitation/inhibition ratio for each cortical area by dividing the mean of the density of all the excitatory receptors by the mean of the inhibitory receptors. Finally, we estimated the changes of the receptor density across cortical areas for ionotropic and metabotropic receptors separately. For the assignment of receptors to the aforementioned categories, that is, excitatory, inhibitory, ionotropic, and metabotropic, see ref. 7. The aforementioned metrics were estimated on a laminar-wise basis. The insights provided by these analyses are detailed in the sections below.

Progressive Molecular Diversity. We associated the entropy of the areas, that is, their receptor diversity, to the primary natural axis. This association was performed on a laminar-wise basis. The analysis reveals that the entropy of areas is aligned with the natural axis. Specifically, for the IG layers the progression

from sensory to association areas along the primary natural axis marked an increase of the entropy and, thus, diversity of receptors (rho = −0.79, $P < 0.01$). This relation was less pronounced for the G layers (rho = −0.42, $P < 0.01$) and statistically absent for the SG layers (rho = −0.13, $P > 0.1$) (Fig. 3*A*). A laminar-wise rank ordering of cortical areas based on their receptor entropy is provided in *SI Appendix*, Fig. S2. These results indicate that the transition from sensory to association areas along the natural axis is accompanied by an increase of the diversity of the receptor profile that an area exhibits. This relation was more prominent in IG layers. We denote this phenomenon as progressive molecular diversity across the primary natural axis of the cerebral cortex. Moreover, there is a tendency of cortical areas at the association end of the natural axis to exhibit the highest entropy values with respect to IG measurements, while the highest entropy measures for cortical areas at the sensory end of the natural axis are observed for SG measurements. We also summarized the entropy of the receptor density across all areas on a laminar-wise basis. The highest entropy was observed for the IG layers, followed by the entropy in the G and SG layers. Statistically significant differences concerned the entropy of the IG receptors when compared to the entropy of the G and SG layers (two-sample Kolmogorov–Smirnov test, 0.45, 0.50, respectively, $P < 0.01$) (Fig. 3*C*).

Progressive Molecular Excitation/Inhibition. We associated the excitation/inhibition of cortical areas to the primary natural axis. This association was performed on a laminar-wise basis. For all layers, the ratio of excitatory to inhibitory receptor density increased along the natural axis when transitioning from sensory to association areas (rho = −0.43, $P < 0.05$ and rho = −0.68, −0.71, $P < 0.01$, for the IG, G, and SG layers,

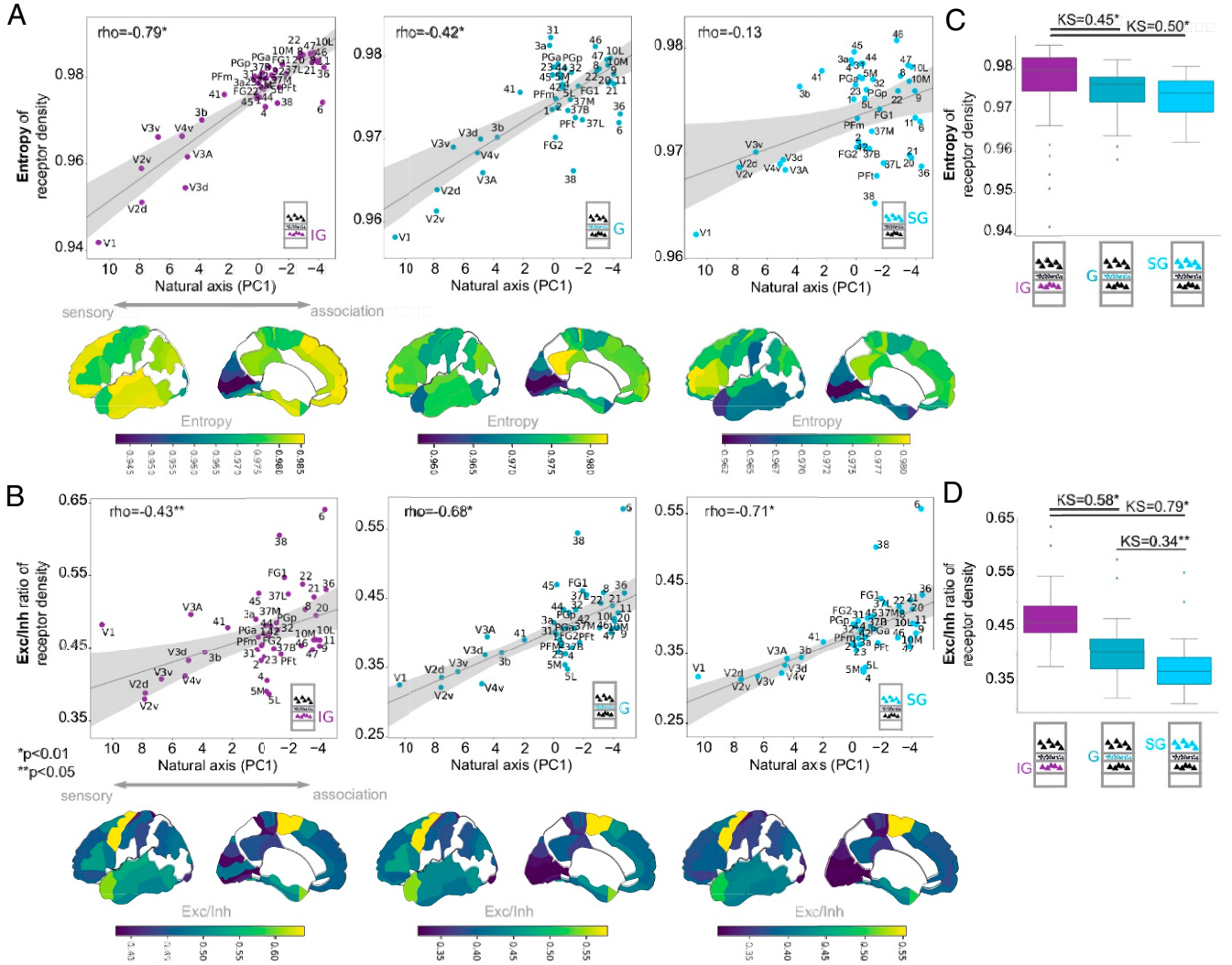

Fig. 3. The principle of progressive molecular diversity and excitatory/inhibitory receptors ratio along the natural axis. (*A*) (*Top*) Diversity of receptor profiles varies along the natural axis (PC1) for each laminar compartment (IG, G, SG). Progressive molecular diversity refers to the increase of the entropy, thus diversity, of the receptor profile of areas when transitioning from sensory to association areas, especially prominent in IG layers. (*Bottom*) Surface maps depict the entropy values across the cerebral cortex. Note the sensory-to-association increase of entropy. (*B*) Same as in *A*, but for the excitatory/inhibitory receptors ratio. The ratio of excitatory/inhibitory receptors increases when transitioning from sensory to association areas, more prominently in SG layers. Note the sensory-to-association increase of the excitatory/inhibitory receptors ratio. (*C*) Entropy of receptor profiles summarized for each laminar compartment (IG, G, SG) for all cortical areas. (*D*) Same as in *C* but for the excitatory/inhibitory receptors ratio. Note that both the overall entropy and excitatory/inhibitory receptors ratio, summarized across all areas, are decreasing across IG, G, and SG layers (*C* and *D*). Note as well that, in this figure only, the *x* axis is ordered in such a way that sensory to association (left to right) transitions entail an increase in the entropy or the excitatory/inhibitory receptors ratio. PC1 values are nonscaled.

respectively) (Fig. 3*B*). A laminar-wise rank ordering of cortical areas based on their excitation/inhibition ratio is provided in *SI Appendix*, Fig. S3. Therefore, the transition from sensory to association areas across the natural axis is accompanied by a progressive increase of the receptor excitation/inhibition ratio of cortical areas. This progressive excitability was more prominent in SG layers. We denote this phenomenon as progressive molecular excitation/inhibition across the primary natural axis of the cerebral cortex. We also summarized the ratio of excitation/inhibition across all areas on a laminar-wise basis. The highest excitation/inhibition ratio was observed for the IG layers, followed by the excitation/inhibition ratio in the G and SG layers. Statistically significant differences concerned the excitation/inhibition ratio of the IG layers when compared to the excitation/inhibition ratio of the G and SG layers (two-sample Kolmogorov–Smirnov test, 0.58, 0.79, respectively, $P < 0.01$), as well as the excitation/inhibition ratio of the G layers when compared to the excitation/inhibition ratio of the SG layers (two-sample Kolmogorov–Smirnov test, 0.34, $P < 0.05$) (Fig. 3*D*).

Mirrored Density Changes of Ionotropic and Metabotropic Transmitter Receptors. We next examined the relation of the density of ionotropic and metabotropic receptors to the primary natural axis. This analysis revealed mirrored changes of the density of the ionotropic and metabotropic receptors along the natural axis. Specifically, ionotropic receptor density increased when transitioning from association to sensory areas with the more prominent, statistically significant increase observed for the SG layers (rho = 0.67, $P < 0.001$). In contrast to the G and SG layers, the density of ionotropic receptors in IG decreased along the natural axis (rho = −0.49, $P < 0.001$) (Fig. 4*A*). The mirrored pattern was observed for the metabotropic receptors for all layers along the natural axis. Specifically, metabotropic receptor density decreased when transitioning from association to sensory areas, with the more prominent decrease observed for the

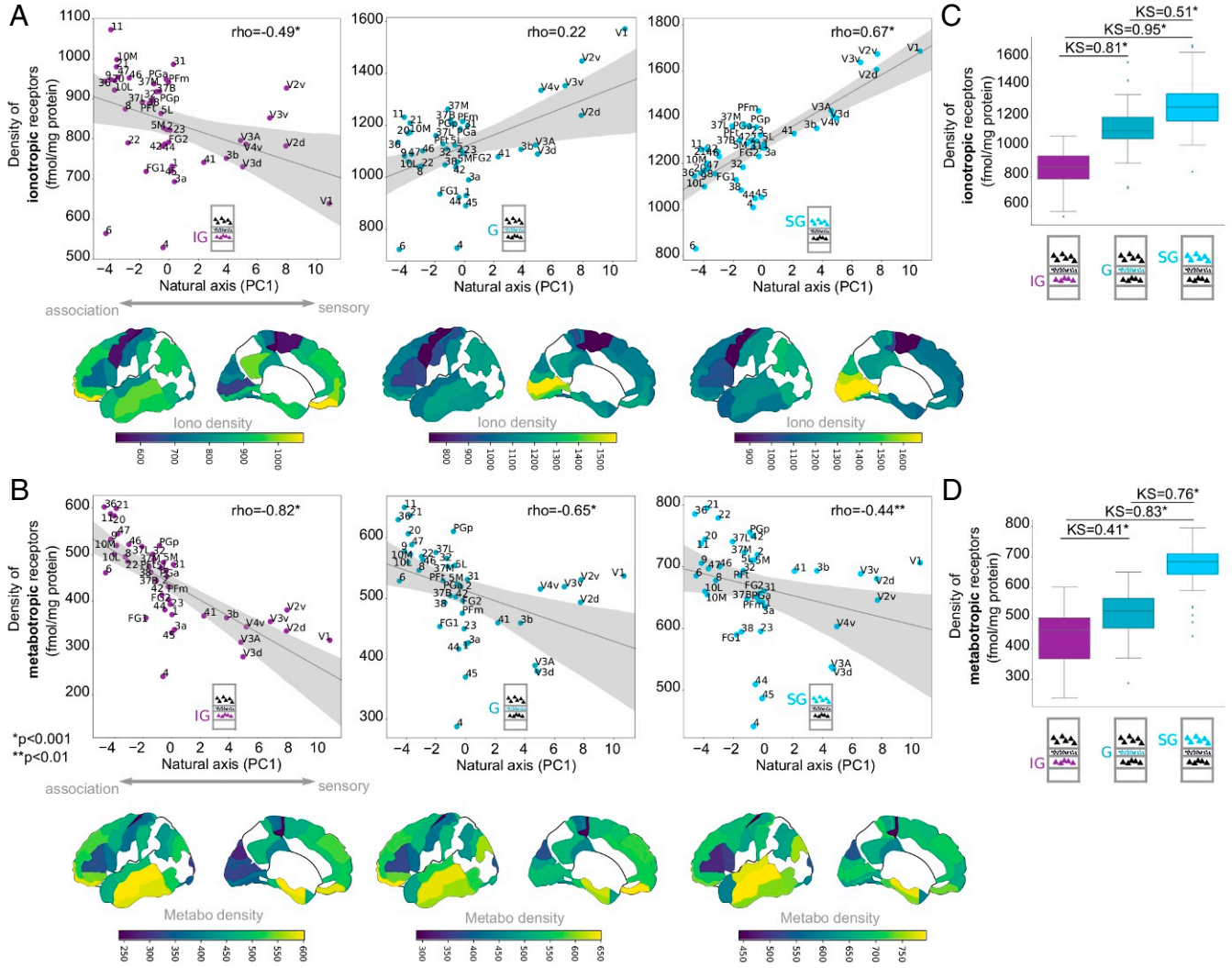

Fig. 4. Mirrored density changes of ionotropic versus metabotropic transmitter receptors along the natural axis (PC1, nonscaled values). (*A*) Density of ionotropic receptors increases in the SG layers when transitioning from sensory to association areas. (*B*) Same as for *A* but for the metabotropic receptors. Note that the metabotropic receptor density exhibits a mirrored pattern along the natural axis when compared to the density of the ionotropic receptors (with the exception of IG layers). Note that there is an increase of metabotropic receptor density when transitioning from sensory to association areas, more prominently in IG layers, whereas there is a decrease of ionotropic receptor density when transitioning from sensory to association areas, more prominently in SG layers. (*C*) Density of ionotropic receptors across all areas summarized for each laminar compartment (IG, G, SG). (*D*) Same as in *C* but for the metabotropic receptors.

IG layers (rho = −0.82, rho = −0.65, $P < 0.001$, rho = −0.44, $P < 0.01$, for the IG, G, and SG layers, respectively) (Fig. 4*B*). A laminar-wise rank ordering of cortical areas based on the density of ionotropic and metabotropic receptors is provided in *SI Appendix*, Fig. S4. In sum, the density of ionotropic receptors, on average, increases when transitioning from association to sensory areas, while the density of metabotropic receptors, on average, decreases. We denote this phenomenon as mirrored density changes of ionotropic and metabotropic receptors along the primary natural axis of the cerebral cortex. Ionotropic receptors form transmembrane ligand-gated ion channels. Metabotropic receptors do not form channels, and their impact on the channels that a cell exhibits relies on signal transduction, that is, a cascade of intracellular events. Hence, on average, the effect of ionotropic receptors on the channels of the cell that they inhabit is faster when compared to the effect of metabotropic receptors. The highlighted differences along the natural axis, thus, have direct functional consequences (*Discussion*).

We also estimated the overall density for ionotropic and metabotropic receptors across cortical areas on a laminar-wise basis. For both metabotropic and ionotropic receptors, an increase in the density was observed across IG, G, and SG. These laminar-wise differences were statistically significant (two-sample Kolmogorov–Smirnov test: ionotropic, 0.81, 0.95, 0.51; metabotropic, 0.41, 0.83, 0.76; for IG versus G, IG versus SG, and G versus SG, respectively; $P < 0.001$) (Fig. 4 *C* and *D*).

Discussion

The Natural Axis of Transmitter Receptor Distribution. Numerous classic (14–18) and more recent studies (19–26) dictate that the heterogeneity of the cerebral cortex of mammals in general, and humans in particular, is not spatially random, but instead manifests as spatially ordered changes (gradation principle in ref. 15). These changes have a characteristic spatial trajectory with sensory areas at one end and association areas at the other end (14, 17, 27). This sensory to association axis also entails more to less laminar differentiation, that is, distinguishability and prominence of the layers of the cerebral cortex, for instance, in terms of cell packing density and/or size of cell bodies (14, 22, 26). Our results highlight that the distribution of transmitter receptor density also follows this spatial trajectory and, thus, forms a natural axis of variation at the molecular level. Therefore, this spatial trajectory at the molecular level is tightly linked with the spatial trajectory that pertains to the myeloarchitectonic (19), cytoarchitectonic (22), and functional (25) dimensions of cortical organization. These associations are yet another manifestation of the principle of concurrent change that pertains to the cerebral cortex; that is, variations of features across the cortical sheet are concurrent and involve multiple dimensions of cortical organization (27).

In particular, our analysis unveils the prominent receptors that drive the segregation of cortical areas along the natural axis. Specifically, glutamate receptors AMPA and NMDA exhibit opposed preferences: NMDA is prominent in the sensory, highly differentiated cortical areas, while AMPA is more prominent in less differentiated cortical areas. Moreover, these opposed preferences manifest in a layer-wise fashion. While the more pronounced NMDA preference toward highly differentiated sensory cortical areas, predominantly the visual areas, involves the SG layers, the more pronounced AMPA preference toward less differentiated association cortical areas involves the IG layers. In other words, the laminar-wise relative preferences of AMPA and NMDA receptors reflect the shifts of the laminar-wise relative preference of termination of interareal connections, as empirical observations in the monkey and cross-species wiring principles dictate (20, 29, 30) (Fig. 5*B*). Such organizational principles substantiate prior suggestions in the context of the modeling of the global neuronal workspace hypothesis (31). These suggestions postulate that top–down connections (association to sensory) are more related to the propensity of NMDA receptors, whereas bottom–up connections (sensory to association) are more related to the propensity of AMPA receptors (31). Thus, the more pronounced NMDA densities in SG layers in visual areas might constitute the molecular signature that facilitates top–down mediated plasticity of these areas. Moreover, our results highlight the prominence of the $GABA_A$, a_2, M2, and D_1 receptors for the highly differentiated sensory cortical areas. Our results complement previous univariate assessments of the density of transmitter receptors and their relation to sensory areas (7). In sum, we reveal the natural axis of transmitter receptor distribution in the human cerebral cortex and the associated contributions of specific receptor types to the segregation of cortical areas along this axis.

Progressive Molecular Diversity, Excitation/Inhibition, and Mirrored Ionotropic/Metabotropic Changes along the Natural Axis. We have highlighted three key organizational principles of the molecular composition of the cerebral cortex that manifest along the natural axis (Fig. 5*A*). The principle of progressive molecular diversity illustrates that the diversity of receptor densities in each area increases when we transition from more differentiated, sensory areas to the less differentiated, association areas. This increase is more pronounced in IG layers. This principle indicates that association areas may exhibit their characteristic diverse functional profile, that is, their engagement in diverse tasks (32, 33), due to their broad tuning at the molecular level that allows them to be modulated by multiple neurotransmitter systems. Therefore, this principle offers cognitive neuroscience insights at the molecular level and generates a concrete prediction; that is, entropy of receptor profiles of cortical areas will be predictive of their functional diversity, above and beyond factors such as connectomic properties of areas (33). Moreover, combining insights from invasive tract-tracing studies in the monkey (30, 34) and cross-species wiring principles (20, 29, 30), we can also predict that, for association areas, the predominant laminar termination of interareal structural connections will involve the IG layers of the human cerebral cortex (Fig. 5*C*). This termination preference mirrors the increased entropy of the molecular profile of IG layers in association areas (Fig. 5*C*). Therefore, we have a synergy between the connectional and receptor levels of organization that bestow the IG layers of association areas with a prominent role in accommodating incoming signals from areas that lie toward the other end of the natural axis. By contrast, the preferential termination in more differentiated, sensory areas involves the SG layers (Fig. 5*B*). SG layers of these areas exhibit low entropy; thus, their molecular profile is specialized and not broad (Fig. 5*C*). In sum, the principle of progressive molecular diversity unifies receptor and connectional features and provides insights into the functional profile of cortical areas at the molecular level.

The principle of progressive excitation/inhibition ratio denotes that the excitation/inhibition ratio of receptor densities increases when we transition from more differentiated, sensory areas to the less differentiated, association areas. Observations in human and nonhuman primates indicate that the spine density of pyramidal cells increases in the transition from sensory to association areas (35). This feature bestows association areas with higher degrees of excitability that may contribute to their integrative functional capacity, as empirical and computational studies indicate (36–38). Moreover, it is noteworthy that the gradual increase of the excitatory to inhibitory receptor density from sensory (more differentiated) to association (less differentiated) areas resembles the decrease of the density of inhibitory neurons as evidence in the macaque monkey cortex indicates, where less differentiated areas exhibit low density of inhibitory neurons and more differentiated areas exhibit high density of inhibitory neurons (39). The principle of

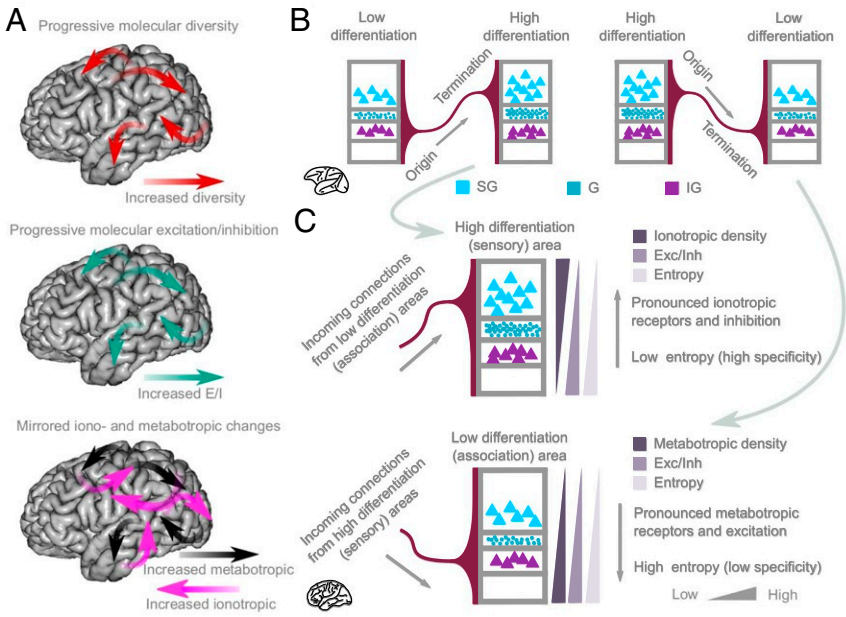

Fig. 5. Organizational principles of receptor distribution and the interareal cortical projection system. (*A*) Summary of organizational principles of receptor distribution along the primary natural axis. Note that this is a schematic representation denoting the overall changes across the sensory to association axis. For detailed results, see Figs. 2–4. (*B*) Wiring principles dictating the predominant origin and termination of cortico-cortical connections in the monkey. Less differentiated areas elicit connections predominantly from deep laminar compartments (IG layers) and when targeting more differentiated areas they terminate predominantly in upper layers (SG layers). The reverse pattern of origin and termination of connections is observed for efferents from more to less differentiated areas. The differentiation of areas is the most consistent explanatory model of the shifts of the laminar connectional patterns (28–30) and can be used for monkey to human extrapolations (20, 29), thus generating predictions for the origin and termination of cortico-cortical connections in the human cerebral cortex. (*C*) Receptor principles across layers for more and less differentiated areas. In more differentiated areas, toward the sensory end of the natural axis, the density of ionotropic receptors increases from deep (IG) to upper (SG) layers. Moreover, entropy and excitatory/inhibitory receptors ratio decreases; thus, a high specificity and an inhibitory nature prevail. These graded changes at the receptor level are aligned with the predominant terminations of connections from less differentiated areas to upper layers, as predicted by the monkey-based model in *B*. In less differentiated areas, toward the association-related end of the natural axis, the density of metabotropic receptors increases from upper (SG) to lower (IG) layers. Moreover, entropy and excitatory/inhibitory receptors ratio increases; thus, a high molecular diversity and an excitatory nature prevail. These graded changes at the receptor level are aligned with the predominant terminations of connections from more differentiated areas to deep layers, as predicted by the monkey-based model in *B*. Thus, the uncovered receptor principles distill insights that can be combined with predictions pertaining to the connectional level to unveil a molecular-connectional synergy in the human cerebral cortex.

progressive increase in the excitatory/inhibitory receptors ratio extends these observations by offering a receptor-based explanation for the pronounced excitability of the neuronal populations inhabiting association areas. Such a principle can be instantiated in computational models embodying regional heterogeneity (36, 40, 41), thus offering enhanced neurobiological interpretability. Notably, the highest excitatory/inhibitory receptors ratio is observed in IG layers (Fig. 5*C*). In monkeys, the predominant termination of interareal connections in association areas involves the IG layers (30) (Fig. 5*B*). Interareal connections, especially connections spanning long distances, are, on average, very weak in terms of the number of axons that they involve, when compared to short-range connections (34, 42). Therefore, the highest excitability of IG may constitute a molecular signature that facilitates these weak, long-range connections to excite their downstream targets in the human cerebral cortex. Advancements in the in vivo mapping of long-range connections in humans may confirm such connectional–molecular synergy in the human cerebral cortex. Note that while here we focus on cortico-cortical connections, our receptor-based principles should also be linked to thalamo-cortical and cortico-thalamic connections. For instance, since IG layers constitute the major origin of cortico-subcortical connections, high excitability of IG may also constitute a molecular signature that is necessary for cortical to subcortical connections. Note as well that the inverse relation of physical distance and connectivity strength is not a perfect linear relation, and thus, certain connections between areas can have a high strength (43), compared to what is expected from the overall inverse relation of distance and strength of connections. Further predictions based on the principle of progressive molecular excitation/inhibition pertain to the functional connectivity properties of cortical areas. In monkeys and humans, prior studies involving a small set of cortical areas highlight a relation between the excitation/inhibition ratio and the functional connectivity strength of areas (44, 45). Thus, the principle of progressive excitation/inhibition ratio constitutes a template for predicting such functional connectivity properties of areas at a global whole-cortex level. From a clinical standpoint, the principle of progressive excitation/inhibition ratio across the cortical sheet may offer explanations and predictions with respect to pathology. For instance, areas with high excitation/inhibition ratio, such as areas 6 and 38, may be situated close to an excitability threshold above which pathological neuronal activity may arise, as is the case in epilepsy. In sum, the principle of progressive excitatory/inhibitory ratio can be instantiated in computational models to offer enhanced neurobiological interpretability and may predict and explain deviant neurophysiological profiles in a clinical context.

Finally, the mirrored ionotropic/metabotropic changes along the natural axis dictate that the density of ionotropic receptors increases when we transition from association to sensory areas, while density of metabotropic receptors exhibits the mirrored pattern, that is, increases when we transition from sensory to association areas. Primary sensory areas operate on fast

temporal scales and the predominant density of ionotropic transmitter receptors may bestow them with this functional property, since the very nature of ionotropic receptors is the presence of ion channels with fast, immediate effects on the cell that they inhabit. On the contrary, association areas are characterized by high density of metabotropic transmitter receptors that have a slower, indirect impact on the cells that they inhabit. This property may bestow these areas with a functional repertoire that operates at slow temporal scales (such as learning processes), possibly accounting for their integrative and coordinating role. Such a suggestion is further supported by empirical studies reporting higher concentrations of the plasticity-related calcium calmodulin-dependent protein kinase II in association areas of the monkey cortex (46). Notably, the increase of metabotropic receptor density toward the end of the natural axis occupied by association areas is more prominent in the IG layers, while the increase of ionotropic receptor density toward the other end of the natural axis occupied by sensory areas is more prominent in the SG layers (Fig. 5 *A* and *C*). Based on observations in the monkey and cross-species wiring principles (20, 29), these changes at the molecular level are centered around the most prominent laminar terminations, and thus incoming signals, of interareal cortical connections (Fig. 5).

Conclusions

We uncovered organizational principles that pertain to the distribution of the density of transmitter receptors in the human cerebral cortex. We demonstrate that receptor densities are organized along a natural axis in the cerebral cortex, ranging from sensory to association areas. The constellation of areas along this axis is characterized by organizational changes that are regulated by the principles of progressive molecular diversity, excitation/inhibition, and mirrored changes of the density of ionotropic and metabotropic receptors. Our results showcase the importance and feasibility of taming the complexity of the cerebral cortex by distilling key organizational principles that bring order to the heterogeneity of cortical organization.

Materials and Methods

Receptor autoradiography data that were used for this study were collected as described in ref. 7. Briefly, receptor densities were quantified by in vitro receptor autoradiographical analysis of four hemispheres from three brains obtained in compliance with the requirements defined by the local ethical committee through the body donor program of the Department of Anatomy, University of Düsseldorf, Düsseldorf, Germany, which also requires written consent by the donor. Donors (two males, one female; 75 $\pm$ 3 y of age; postmortem delay 12 $\pm$ 5 h) had no record of neurological or psychiatric diseases, and causes of death were cardiac arrest, lung edema, and myocardial infarction. A postmortem stability of up to 70 to 80 h has been described for neurotransmitter binding-site densities, and significant decreases occur mainly as from 27 h, with the exception of muscarinic binding sites, for which a loss of up to 10% was found within the first 20 h (for a review see ref. 47). For details see ref. 7. For analyses and metrics used, see *SI Appendix, SI Text*.

Data Availability. Anonymized receptor autoradiography data and Python code used for the analysis and figures have been deposited in GitHub (https://github.com/AlGoulas/receptor_principles).

ACKNOWLEDGMENTS. Funding from the European Union's Horizon 2020 Research and Innovation Program, Grants 604102 (HBP, SGA1) (to K.A.), 785907 (HBP SGA2) (to K.A., N.P.-G., C.C.H., J.-P.C.), and 945539 (HBP SGA3) (to K.A., N.P.-G., C.C.H., and J.-P.C.), as well as funding from the Deutsche Forschungsgemeinschaft (SFB 936/A1, TRR 169/A2, SPP 2041/HI 1286/7-1, HI 1286/6-1) (to C.C.H.), is gratefully acknowledged.

1. M. R. Bennett, The concept of transmitter receptors: 100 years on. *Neuropharmacology* **39**, 523–546 (2000).
2. F. K. Bedford *et al.*, GABAa receptor cell surface number and subunit stability are regulated by the ubiquitin-like protein Plic-1. *Nat. Neurosci.* **4**, 908–916 (2001).
3. A. Nieoullon, Dopamine and the regulation of cognition and attention. *Prog. Neurobiol.* **67**, 53–83 (2002).
4. J. P. Changeux, Allosteric receptors: From electric organ to cognition. *Annu. Rev. Pharmacol. Toxicol.* **50**, 1–38 (2010).
5. I. Shimada, T. Ueda, Y. Kofuku, M. T. Eddy, K. Wüthrich, GPCR drug discovery: Integrating solution NMR data with crystal and cryo-EM structures. *Nat. Rev. Drug Discov.* **18**, 59–82 (2019).
6. K. Zilles, K. Amunts, Receptor mapping: Architecture of the human cerebral cortex. *Curr. Opin. Neurol.* **22**, 331–339 (2009).
7. K. Zilles, N. Palomero-Gallagher, Multiple transmitter receptors in regions and layers of the human cerebral cortex. *Front. Neuroanat.* **11**, 78 (2017).
8. M. L. Kringelbach *et al.*, Dynamic coupling of whole-brain neuronal and neurotransmitter systems. *Proc. Natl. Acad. Sci. U.S.A.* **117**, 9566–9576 (2020).
9. J. Ceccarini, H. Liu, K. Van Laere, E. D. Morris, C. Y. Sander, Methods for quantifying neurotransmitter dynamics in the living brain with PET imaging. *Front. Physiol.* **11**, 792 (2020).
10. V. Beliveau *et al.*, A high-resolution in vivo atlas of the human brain's serotonin system. *J. Neurosci.* **37**, 120–128 (2017).
11. R. Cortes, A. Probst, H. J. Tobler, J. Palacios, Muscarinic cholinergic receptor subtypes in the human brain. II. Quantitative autoradiographic studies. *Brain Res.* **362**, 239–253 (1986).
12. K. Amunts *et al.*, Broca's region: Novel organizational principles and multiple receptor mapping. *PLoS Biol.* **8**, e1000489 (2010).
13. N. Palomero-Gallagher, K. Zilles, Cortical layers: Cyto-, myelo-, receptor- and synaptic architecture in human cortical areas. *Neuroimage* **197**, 716–741 (2019).
14. C. F. von Economo, G. N. Koskinas, *Die Cytoarchitektonik der Hirnrinde des Erwachsenen Menschen* (Julius Springer Verlag, Vienna, Austria; Berlin, Germany, 1925).
15. F. Sanides, *Die Architectonik des Menschlichen Stirnhirns* (Springer-Verlag, Berlin-Heidelberg, Germany, 1962).
16. A. A. Abbie, Cortical lamination in the monotremata. *J. Comp. Neurol.* **72**, 429–467 (1940).
17. D. N. Pandya, E. H. Yeterian, "Architecture and connections of cortical association areas" in *Cerebral Cortex Vol.4 Association and Auditory Cortices*, A. Peters, E. G. Jones, Eds. (Springer US, Boston, MA, 1985), pp. 3–61.
18. R. Nieuwenhuys, The myeloarchitectonic studies on the human cerebral cortex of the Vogt-Vogt school, and their significance for the interpretation of functional neuroimaging data. *Brain Struct. Funct.* **218**, 303–352 (2013).
19. J. B. Burt *et al.*, Hierarchy of transcriptomic specialization across human cortex captured by structural neuroimaging topography. *Nat. Neurosci.* **21**, 1251–1259 (2018).
20. A. Goulas, K. Zilles, C. C. Hilgetag, Cortical gradients and laminar projections in mammals. *Trends Neurosci.* **41**, 775–788 (2018).
21. B. D. Fulcher, J. D. Murray, V. Zerbi, X. J. Wang, Multimodal gradients across mouse cortex. *Proc. Natl. Acad. Sci. U.S.A.* **116**, 4689–4695 (2019).
22. C. Paquola *et al.*, Microstructural and functional gradients are increasingly dissociated in transmodal cortices. *PLoS Biol.* **17**, e3000284 (2019).
23. B. Zikopoulos, M. A. Garcia-Cabezas, H. Barbas, Parallel trends in cortical gray and white matter architecture and connections in primates allow fine study of pathways in humans and reveal network disruptions in autism. *PLoS Biol.* **16**, e2004559 (2018).
24. J. M. Huntenburg, P. L. Bazin, D. S. Margulies, Large-scale gradients in human cortical organization. *Trends Cognit. Sci.* **22**, 21–31 (2018).
25. D. S. Margulies *et al.*, Situating the default-mode network along a principal gradient of macroscale cortical organization. *Proc. Natl. Acad. Sci. U.S.A.* **113**, 12574–12579 (2016).
26. K. Wagstyl *et al.*, Bigbrain 3D atlas of cortical layers: Cortical and laminar thickness gradients diverge in sensory and motor cortices. *PLoS Biol.* **18**, 1–21 (2020).
27. C. C. Hilgetag, S. F. Beul, S. J. van Albada, A. Goulas, An architectonic type principle integrates macroscopic cortico-cortical connections with intrinsic cortical circuits of the primate brain. *Network Neurosci.* **3**, 905–923 (2019).
28. S. F. Beul, C. C. Hilgetag, Neuron density fundamentally relates to architecture and connectivity of the primate cerebral cortex. *Neuroimage* **189**, 777–792 (2019).
29. A. Goulas, P. Majka, M. G. P. Rosa, C. C. Hilgetag, A blueprint of mammalian cortical connectomes. *PLoS Biol.* **17**, e2005346 (2019).
30. H. Barbas, N. Rempel-Clower, Cortical structure predicts the pattern of corticocortical connections. *Cerebr. Cortex* **7**, 635–646 (1997).
31. S. Dehaene, J. P. Changeux, Experimental and theoretical approaches to conscious processing. *Neuron* **70**, 200–227 (2011).
32. B. T. T. Yeo *et al.*, Functional specialization and flexibility in human association cortex. *Cerebr. Cortex* **25**, 3654–3672 (2014).
33. M. Najafi, B. W. McMenamin, J. Z. Simon, L. Pessoa, Overlapping communities reveal rich structure in large-scale brain networks during rest and task conditions. *Neuroimage* **135**, 92–106 (2016).
34. N. T. Markov *et al.*, Anatomy of hierarchy: Feedforward and feedback pathways in macaque visual cortex. *J. Comp. Neurol.* **522**, 225–259 (2014).

35. G. N. Elston, I. Fujita, Pyramidal cell development: Postnatal spinogenesis, dendritic growth, axon growth, and electrophysiology. *Front. Neuroanat.* **8**, 78 (2014).
36. R. Chaudhuri, K. Knoblauch, M. A. Gariel, H. Kennedy, X. J. Wang, A large-scale circuit mechanism for hierarchical dynamical processing in the primate cortex. *Neuron* **88**, 419–431 (2015).
37. C. Honey *et al.*, Slow cortical dynamics and the accumulation of information over long timescales. *Neuron* **76**, 423–434 (2012).
38. U. Hasson, E. Yang, I. Vallines, D. J. Heeger, N. Rubin, A hierarchy of temporal receptive windows in human cortex. *J. Neurosci.* **28**, 2539–2550 (2008).
39. S. Dombrowski, C. Hilgetag, H. Barbas, Quantitative architecture distinguishes prefrontal cortical systems in the rhesus monkey. *Cerebr. Cortex* **11**, 975–988 (2001).
40. M. Demirtas *et al.*, Hierarchical heterogeneity across human cortex shapes large-scale neural dynamics. *Neuron* **101**, 1181–1194.e13 (2019).
41. G. Deco *et al.*, Whole-brain multimodal neuroimaging model using serotonin receptor maps explains non-linear functional effects of LSD. *Curr. Biol.* **28**, 3065–3074.e6 (2018).
42. N. T. Markov *et al.*, Cortical high-density counterstream architectures. *Science* **342**, 1238406 (2013).
43. C. Cavada, P. S. Goldman-Rakic, Posterior parietal cortex in rhesus monkey: II. Evidence for segregated corticocortical networks linking sensory and limbic areas with the frontal lobe. *J. Comp. Neurol.* **287**, 422–445 (1989).
44. E. Turk, L. H. Scholtens, M. P. van den Heuvel, Cortical chemoarchitecture shapes macroscale effective functional connectivity patterns in macaque cerebral cortex. *Hum. Brain Mapp.* **37**, 1856–1865 (2016).
45. M. P. van den Heuvel *et al.*, Multimodal analysis of cortical chemoarchitecture and macroscale fMRI resting-state functional connectivity. *Hum. Brain Mapp.* **37**, 3103–3113 (2016).
46. M. Garcia-Cabezas, M. K. P. Joyce, Y. J. John, B. Zikopoulos, H. Barbas, Mirror trends of plasticity and stability indicators in primate prefrontal cortex. *Eur. J. Neurosci.* **46**, 2392–2405 (2017).
47. N. Palomero-Gallagher, K. Amunts, K. Zilles, "Transmitter receptor distribution in the human brain" in *Brain Mapping: An Encyclopedic Reference Vol. 2*, A. W. Toga, Ed. (Elsevier Academic Press, San Diego, CA, 2015), pp. 261–275.